PROTEINS: Structure, Function, and Genetics 40:249–257 (2000)

Crystal Structure of Recombinant Trypsin-Solubilized Fragment of Cytochrome b_5 and the Structural Comparison With Val61His Mutant

JianWu,[1] Jian-Hua Gan,[1] Zong-Xiang Xia,[1*] Yun-Hua Wang,[2] Wen-Hu Wang,[2] Ling-Long Xue,[2] Yi Xie,[2] and Zhong-Xian Huang[2]

[1]*State Key Laboratory of Bio-Organic and Natural Products Chemistry, Shanghai Institute of Organic Chemistry, Chinese Academy of Sciences, Shanghai, China*

[2]*Chemical Biology Laboratory, Department of Chemistry, Fudan University, Shanghai, China*

ABSTRACT **The crystal structure of the recombinant trypsin-solubilized fragment of the microsomal cytochrome b_5 from bovine liver has been determined at 1.9 Å resolution and compared with the reported crystal structure of the lipase-solubilized fragment of the membrane protein cytochrome b_5. The two structures are similar to each other. However, some detailed structural differences are observed: the conformation of the segment Asn16–Ser20 is quite different, some helices around the heme and some segments between the helices are shifted slightly, the heme is rotated about the normal of the mean plane of heme, one of the propionates of the heme exhibits a different conformation. The average coordination distances between the iron and the two nitrogen atoms of the imidazole ligands are the same in the two structures. Most of the structural differences can be attributed to the different intermolecular interactions which result from the crystal packing. The wild-type protein structure is also compared with its Val61His mutant, showing that the heme binding and the main chain conformations are basically identical with each other except for the local area of the mutation site. However, when Val61 is mutated to histidine, the large side chain of His61 is forced to point away from the heme pocket toward the solvent region, disturbing the micro-environment of the heme pocket and influencing the stability and the redox potential of the protein. Proteins 2000;40:249–257.**

Key words: cytochrome b_5; trypsin-cleaved fragment; recombinant wild type; crystal structure; structure comparison with lipase-cleaved fragment; mutant Val61His

INTRODUCTION

Cytochromes are a diverse group of proteins that widely exist in bacteria, protozoa, yeast, and higher organisms, and they are divided on a structural basis into four major families, all of which contain heme group.[1]

Microsomal cytochrome b_5 is a member of the cytochrome b_5 family, located in a variety of cell types and intracellular sites, such as liver cells of mammals and avian species.[2] It serves as an electron-transfer component involved in a series of electron transfer processes in biological systems. For example, it functions as a member of a three-component electron transport enzyme system to desaturate fatty acids and as a reductant for cytochrome P450, and it also catalyzes the reduction of methemoglobin.[1]

Microsomal cytochrome b_5 is a transmembrane protein with $M_r \sim 16$ KDa,[3] and it consists of two domains: a hydrophilic domain and a hydrophobic one, containing approximately 100 and 30 amino acid residues, respectively.[4] The hydrophilic domain containing the heme group is responsible for the biological activities, while the hydrophobic one for the binding of the protein to the membrane. Proteolyzed by trypsin and lipase, cytochrome b_5 produces the soluble N-terminal fragments consisting of 84 residues (Ala3-Lys86) and 93 residues (Ser1-Ser93), which are referred to as Tb_5 and Lb_5, respectively.[2]

The crystal structure of Lb_5 from bovine liver up to 1.5 Å resolution[2,5–7] was previously reported, which revealed the three-dimensional structure of the protein and the heme binding details. Based on Lb_5 structure, the models for the interaction between cytochrome b_5 and its electron transfer partner cytochrome c were proposed.[8–10] Recently, the crystal structure of the soluble fragment of mitochondrial outer membrane cytochrome b_5 (referred to as OMb_5) from rat liver was determined at 2.7 Å resolution[11] showing that its overall structure is similar to that of Lb_5, and the crystal structure of a double mutant of OMb_5, Val45Leu/Val61Leu, was also reported.[12]

Up to date there was no report yet on the crystal structure of Tb_5. We recently determined the crystal structure of a Val61His mutant of Tb_5 at 2.1 Å resolution.[13] The Val61His structure shows some structural features different from the reported Lb_5 structure.[13] In

Grant sponsor: National Program of Space Application; Grant sponsor: National Key Laboratory of Bio-organic and Natural Product Chemistry of China of Shanghai Institute of Organic Chemistry; Grant sponsor: National Natural Science Foundation.

Atomic coordinates have been deposited with Brookhaven Protein Data Bank: 1EHB (wild-type Tb5) and 1ES1 (Val61His mutant).

*Correspondence to: Zong-Xiang Xia, Shanghai Institute of Organic Chemistry, 354 Fenglin Road, Shanghai 200032, China. E-mail: xiazx@pub.sioc.ac.cn

Received 15 November 1999; Accepted 31 January 2000

order to elucidate whether these differences result from the mutation or from the differences in the lengths of the polypeptide and in the crystal packing between Tb_5 and Lb_5, we have determined the crystal structure of the recombinant wild-type Tb_5 at 1.9 Å resolution. In addition, the Val61His mutant structure has been improved by further refinement using a more powerful program package. In this paper we report the preparation of recombinant Tb_5, present its crystal structure, and compare it with those of Lb_5 and the Val61His mutant of Tb_5. The structure comparison of Tb_5 with other homologous proteins is also discussed.

MATERIALS AND METHODS

Materials

DNA restriction endonucleases, T4 DNA polymerase, ligase and kinase were purchased from Biolabs. [γ-^{32}P]ATP was from Amersham (Arlington Heights, IL). The pUC19 plasmid containing the synthetic gene encoding the trypsin-solubilized bovine liver microsomal cytochrome Tb_5 (82 residues in length, Ala3-Arg84) was a generous gift of Professor A. G. Mauk.[14] The other bio-products were from Sino-American Biotechnology Co. All chemicals were of reagent grade.

Construction of Cytochrome Tb_5 Val61His Mutant Gene

Unless specified, all DNA manipulations were performed as described by Sambrook et al.[15] Site-directed mutagenesis of the gene coding for the trypsin-solubilized cytochrome b_5 was accomplished by using phage M13mp19 as described by Sambrook et al.[15] The oligonucleotide mixture was purified by polyacrylamide gel electrophoresis under non-denaturing condition, followed by reverse-phase liquid chromatography with a C18 cartridge. The mutated cytochrome b_5 genes were sequenced by the dideoxynucleotide chain termination method[16] and then ligated into EcoR I/Hind III cut pUC19 and transformed into *E. coli* host cell JM83.

Preparation of Recombinant Cytochrome Tb_5 and Val61His Mutant Protein

The bacteria containing the genes of wild-type and mutated cytochrome Tb_5 were cultured, harvested with centrifugation, and sonicated. Then the proteins were isolated and purified by ammonium sulfate precipitation, DEAE-DE52 ion-exchange chromatography and Sephedex G75 gel filtration. The purified proteins with $A_{412}/A_{280} > 5.7$ were lyophilized and stored at -70°C. The purity of the proteins was characterized by SDS-PAGE and amino acid analysis. The determination of molecular weights of the proteins was performed on a Quattro MS/MS Electrospray mass spectrometer (VG, United Kingdom). The molecular weights of wild-type and Val61His mutant of cytochrome Tb_5 are 9461.5 ± 1.3 and 9498.9 ± 2.0, respectively, which agree with the molecular weights calculated from the amino acid compositions of apo-cytochrome Tb_5 (9461.3 and 9499.0, respectively). These results confirmed the completely successful mutagenesis and high purity of the proteins.

TABLE I. Crystal Data and Data Collection Statistics

Space Group	C2
Cell dimensions	
a (Å)	70.70
b (Å)	40.44
c (Å)	39.28
β (°)	111.76
Number of molecules per asymmetric unit	1
V_M (Å^3/Da)	2.61
Resolution range (Å)	100.0–1.9
Number of unique reflections	7783
R_{sym} (%)[a]	6.0 (21.0)[b]
Data completeness (%)	94.3 (92.6)[b]
$\langle I/\sigma(I)\rangle$[c]	18.2 (7.3)[b]

[a] R_{sym} = SUM (ABS (I-<I>))/SUM (I).
[b] The numbers in the parentheses correspond to the data in the highest resolution shell (1.90–1.94 Å).
[c] Mean signal-to-noise ratio.

Crystallization and X-Ray Data Collection

Single crystals of Tb_5 were grown in hanging drops using the vapor diffusion method by mixing 5 µl of the reservoir solution (3.2 M phosphate buffer, pH 8.0) with 5 µl of the protein solution (20 mg/ml recombinant Tb_5) at 20°C. The crystallizing conditions are similar to those used for Lb_5 crystallization.[5] The crystals grew to dimensions of 0.6 mm × 0.5 mm × 0.3 mm within a week. The crystals belong to monoclinic space group C2 with unit cell parameters a = 70.70 Å, b = 40.44 Å, c = 39.28 Å, and $\beta = 111.76$°. There is one molecule per asymmetric unit, with a V_M[17] of 2.61 Å^3/dalton. Table I lists the crystal data of Tb_5.

The X-ray data were collected up to 1.9 Å resolution using one single crystal on a MarResearch Imaging Plate-300 Detector system. The data were processed using the programs DENZO and SCALEPACK[18], giving an R_{sym} of 6.0% and data completeness of 94.3%. The data collection statistics are also shown in Table I.

Structure Determination and Refinement

The structure determination and refinement of the Tb_5 structure were carried out using the program packages X-PLOR[19] and CNS[20] successively on a Silicon Graphics Indigo 2 workstation. All the data up to 1.9 Å were used to refine the structure in the CNS refinement stage. Ten percent of the data were randomly selected as the test data set used for cross validation. Model building was performed using the graphics software TURBO-FRODO.[21]

The initial structure of Tb_5 was determined by applying difference Fourier method based on the structure of a Phe35Tyr mutant (unpublished results) of Tb_5 at 1.8 Å resolution, which was previously determined using the same method based on the Val61His mutant structure.[13] The rigid body refinement was carried out, leading to an R factor of 25.3% at 2.2 Å resolution. The structure was then refined for both atomic positions and temperature factors for a number of rounds using X-PLOR. It was further

TABLE II. Refinement Statistics

Number of amino acid residues	82
Number of prosthetic group	1
Number of solvent molecules	70
Number of reflections used	7408
R-factor (%)	19.8
Free R-factor (%)	24.8
r.m.s.d.[a]	
Bond lengths (Å)	0.010
Bond angles (°)	1.106
Mean temperature factors (Å^2)	
Main chain	21.07
Side chain	24.42
Heme	22.73
Solvent	40.50

[a]Root-mean-square deviation.

refined using CNS, and the restraint for the iron-histidine ligand coordination distance was set to 2.2 Å. During the refinement, the (2Fo-Fc) and (Fo-Fc) electron density maps were regularly calculated and used for manually rebuilding the model. When the resolution was gradually extended up to 2.0 Å, solvent molecules were gradually included in the model. Only those solvent molecules with temperature factors lower than 50 Å^2 and hydrogen bonded to the protein atoms directly or through other solvent molecules were included in the final model. The simulated-annealing refinement starting from 2500 K at a cooling rate of 25 K per cycle was applied at late stage to remove the model bias possibly introduced during the refinement.

In addition, CNS was used to further refine the Val61His mutant structure[13] in the same way to give the final structural model of this mutant.

RESULTS

Quality of Structure

The R factor and R_{free} of the final model are 19.8% and 24.8%, respectively. The r.m.s. deviations of the bond lengths and bond angles from the ideal values are 0.010 Å and 1.106°, respectively. The refinement statistics are summarized in Table II.

The Ramachandran plot of the refined model shows that all of the non-glycine residues are located within the allowed regions, with 94.4% in the most favored region validated using the program PROCHECK.[22] The Luzzati plot[23] shows that the estimated error of the atomic coordinate is approximately 0.22 Å.

Overall Structure of Tb_5 Molecule

The final model of each Tb_5 molecule contains 82 amino acid residues, one heme group, and 70 solvent molecules

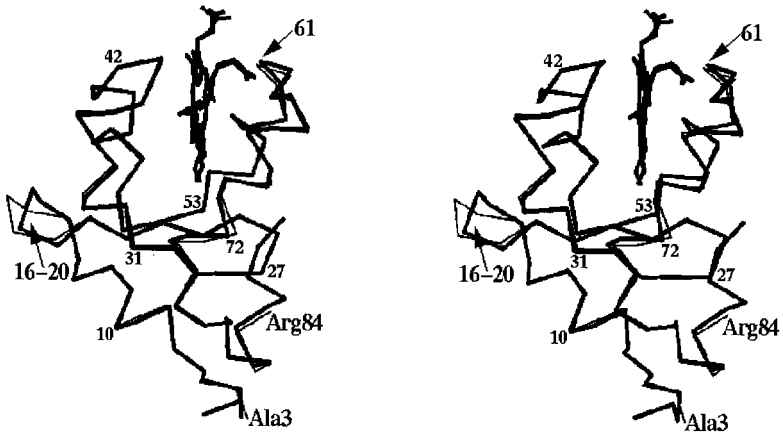

Fig. 1. Cα backbone and the heme of Tb_5, superimposed with those of Lb_5. Tb_5 is shown in thin line and Lb_5 in thick line. Ala3, Arg84, and the segment Asn16–Ser20 are indicated. The Cα atom of the residue Val61 is labeled. Some other residue numbers are labeled to help follow the Cα trace.

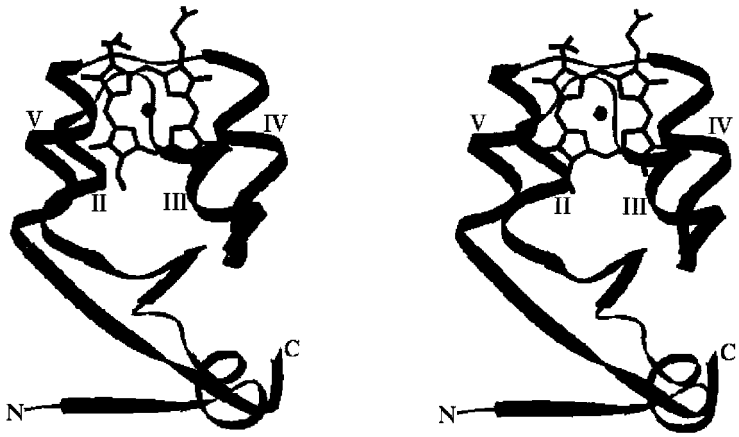

Fig. 2. Ribbon diagram of Tb_5 molecule showing the secondary structure. Heme is also shown. N- and C-termini are indicated. The helices II–V are labeled.

TABLE III. Secondary Structure of Tb_5

a: α-Helices[a,b]

Helix	Starting/ending residues	Irregularity
I	Thr8-His15	O10 interacts with the side chain of Gln13, Glu11-His15 is in 3_{10} helical conformation
II	Leu32-His39	O33 and O34 interacts with two water molecules instead of with main chain nitrogen
III	Glu43-Ala50	The hydrogen bond from O45 to N49 is broken
IV	Ala54-Val61	
V	Ser64-Ile75	O68 interacts with Ser71 OG; Leu70-Ile75 is in 3_{10} helical conformation
VI	His80-Arg84	3_{10} helix

(b) β-sheet

Strand	Starting/ending residues	Relationship between strands n and n-1[c]
I	Lys5-Tyr7	0
II	Thr21-Leu25	+1
III	Tyr27-Leu32	−1
IV	Gly51-Ala54	−1
V	Phe74-His80	+1

[a]Helices are identified based on the hydrogen-bonding pattern.
[b]3_{10} helices are indicted.
[c]+1: strand n parallel to strand n-1; −1: strand n antiparallel to strand n-1; the β-strands are arranged in the order of I-V-III-II-IV.

(Wat301–Wat370). Figure 1 shows the Cα backbone of Tb_5 molecule superimposed with that of Lb_5, indicating that the overall structure of Tb_5 is similar to that of Lb_5. The r.m.s. deviation of the 82 Cα atoms between the two molecules is 0.50 Å. The overall structures of the wild-type and Val61His mutant of Tb_5 are much more similar to each other, with an r.m.s. deviation of 0.10 Å for Cα atoms.

Each Tb_5 molecule contains six helices and one β-sheet composed of five β-strands, as shown in Figure 2 and Table III. The secondary structure of Tb_5 is very similar to that of Lb_5,[7] especially the β-sheet. However, helix IV is slightly longer in Tb_5 than that in Lb_5, and helix VI in Tb_5 structure is obviously shorter than that in Lb_5 since the polypeptide is shorter in Tb_5 at its C-terminus. The irregularity of the hydrogen bonding patterns (Table III) is similar to that of Lb_5,[7] but some differences in the detailed irregularity between the two structures are observed. For example, in helix I the hydrogen bonds from the carbonyl oxygen of Glu10 to the main chain nitrogen of Gln13 are broken in both structures; however, Glu10 O is hydrogen bonded to the side chain of Gln13 in Tb_5 but to a water molecule in Lb_5 structure.

The tertiary structures of Tb_5 and Lb_5 are also similar to each other, as shown in Figure 1. In addition to the amino- and carboxyl-terminal regions of the proteins, the greatest difference between the Tb_5 and Lb_5 structures is observed in the conformation of the segment Asn16–Ser20, the largest deviation being 2.7 Å.

Helix II, helix V, and the C-terminal segment of helix IV exhibit significant shifts compared with those of Lb_5, and the β-turn between helix II and helix III as well as the loop between helix IV and helix V is also somewhat shifted. The conformations of some of the side chains in the molecular surface region of Tb_5 also differ greatly from those of Lb_5, such as Lys5, Leu9, Glu11, Gln13, Glu43, and Arg68.

The structural comparison of the wild-type Tb_5 with its Val61His mutant indicates that the secondary and tertiary structures of them are basically identical with each other except for some slight difference in the main chain conformation in the local area of the mutation site, the segment Phe58-Gly62. The side chains of Val61 in the wild-type Tb_5 and His61 in the Val61His mutant are shown in Figure 3. In the wild-type Tb_5 structure, Val61 is located in the heme-exposed edge region and this side chain points toward the heme group. However, when this residue is mutated to the large residue histidine, the side chain is forced to point away from the heme pocket toward the solvent region to avoid unreasonably close contacts with heme. The main- and side-chain atoms of His61 form three hydrogen bonds to the main chain oxygen atom of Asn57 and two water molecules,[13] helping stabilize the mutated side chain orientation.

Heme Group and Its Environment

The position of the heme in the Tb_5 structure is shown in Figures 1 and 2, which is basically the same as those in the Lb_5 and Val61His structures.[7,13] The heme is located in a hydrophobic pocket. Four helices surround the heme,

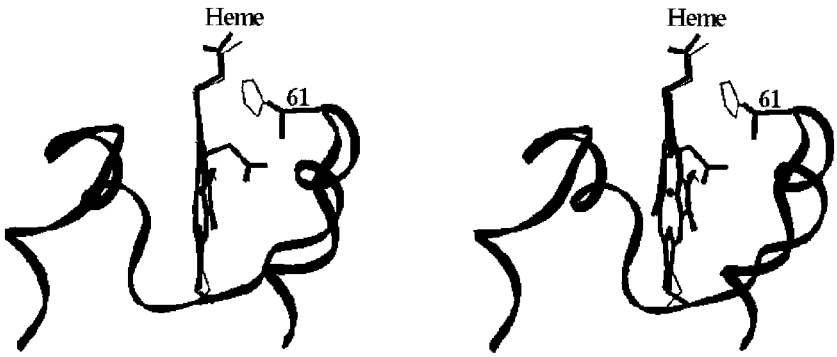

Fig. 3. The heme pocket of Tb_5. The side chain of Val61 is shown in thick line. The side chain of His61 of Val61His mutant is shown in thin line.

three β-strands form the bottom of the heme pocket, and the top part of the heme is exposed to the aqueous environment.

Figure 4a,b shows the final model and the (2Fo-Fc) electron density of the heme of the Tb_5 structure in two different views. Figure 4c,d shows the heme of Tb_5, superimposed with those of Lb_5 and Val61His, also in two different views. The two axial ligands His39 and His63 of the three structures are also superimposed and shown in Figure 4d.

The heme orientation of Tb_5 exhibits a rotation of a few degrees about the normal of the mean plane of the heme from that of Lb_5, while it is very similar to that in the Val61His mutant structure, which is shown in Figure 4c.

The iron is coordinated to four pyrrole nitrogen atoms and two side chains of His39 and His63, as shown in Figure 4c,d. In the Tb_5 structure the coordination distances between Fe and atoms NE2 of His39 and His63 are 2.06 Å and 2.03 Å respectively, which are similar to those in the Lb5 structure (2.04 Å on the average) but 0.05 Å shorter than those in the Val61His mutant structure (2.10 Å on the average). The distances between the Cα atoms and between the NE2 atoms of the two histidine ligands in Tb_5 are also similar to those in Lb_5 and the Val61His mutant structures. The distances and angles relating to the iron coordination are shown in Table IVa.

In each of the Tb_5, Lb_5 and Val61His mutant structures, one of the two propionates interacts with the main- and side-chain atoms of Ser64 through hydrogen bonds, whereas the other propionate fully extends into the solvent region (Figs. 1, 3). The conformation of the former propionate is conserved; however, the latter one shows different conformations in the three structures (Fig. 4c,d). The latter propionate does not form any hydrogen bond with the protein atoms in the wild-type and Val61His mutant of Tb_5, but it is hydrogen bonded to two solvent molecules in the Lb_5 structure.[7]

In the Tb_5 structure, heme forms only one hydrogen bond to the solvent molecule Wat319, which is involved in a solvent network (Table IVb). Three solvent molecules make a bridge between the Tb_5 molecule at X, Y, Z and its symmetry-related molecule at $-X+1/2$, $Y+1/2$, $-Z$. This solvent network does not exist in the Lb_5 structure, and one of the three solvent molecules is well conserved in the Val61His structure while the other two are somewhat shifted in the mutant structure.

Crystal Packing

The intermolecular interactions of Tb_5 are shown in Table V and Figure 5. Each Tb_5 molecule makes contacts with three symmetry-related molecules. The amino-terminal segment of a Tb_5 molecule packs against a symmetry-related molecule, forming four intermolecular hydrogen bonds to the amino-terminal segment and an additional hydrogen bond to a residue of the carboxyl-terminal segment of the latter molecule. The β-turn Asn16–Ser20 interacts with helix I and helix VI of another symmetry-related molecule. Helix II forms hydrogen bonds to the main chain of the loop between helix IV and helix V as well as a residue from β-strand II of the third symmetry-related molecule. Some solvent molecules play roles in bridging symmetry-related molecules.

DISCUSSION

The Crystal Packing Accounts for the Structural Differences Between Tb_5 and Lb_5

Although the overall structure of Tb_5 is similar to that of Lb_5, there are some significant differences between the two structures, which can be ascribed to the different intermolecular interactions resulting from the different crystal packing of the two structures: Tb_5 in space group C2 and Lb_5 in $P2_12_12_1$.

The segments Asn16-Ser20 form β-turns in both Tb_5 and Lb_5 structures. However, they exhibit the greatest difference in the polypeptide chain conformations between Tb_5 and Lb_5 molecules. This segment forms five intermolecular hydrogen bonds from the main chain and side chain of Ser18 to a symmetry-related molecule in Tb_5 (Table V), but only two intermolecular hydrogen bonds from the side chain of Asn16 in an Lb_5 molecule to a symmetry-related molecule.[7] The temperature factors of this segment are lower in Tb_5 than those in Lb_5 structure,[7] i.e., the B values of only three main chain atoms of this segment are higher than 20 $Å^2$ (the highest B = 21.9 $Å^2$) in Tb_5, whereas the B value of the main chain atoms of Asn17, Ser18, and Lys19 are around 30 $Å^2$ in Lb_5. This fact indicates that this segment is more rigid in Tb_5 than that in Lb_5 structure.

Helix V and the C-terminal segment of helix IV of Lb_5 molecule interact with its symmetry-related molecule. However, no intermolecular hydrogen bond interaction exists between the corresponding helices of Tb_5 molecule and its symmetry-related molecule. Although helix II as well as the loop between helix IV and helix V in both Tb_5 and Lb_5 molecules make hydrogen bond interactions with their symmetry-related molecules, the detailed interactions are also different from each other. These different intermolecular interactions result in the significant shifts of helices II, V as well as the segments between helices II and III, between helices IV and V, which are described above.

The Cα atoms of His39 and His63 are located, respectively, in the C-terminus of helix II and in the loop between helix IV and helix V. As discussed above, these segments of Tb_5 are significantly shifted when they are compared with Lb_5 structure, leading to a difference of 0.14 Å in the distances between the Cα atoms of the two axial ligands in the two structures (11.80 Å and 11.66 Å for Tb_5 and Lb_5, respectively; Table IVa). The side chain conformations of the axial ligands His63 differ from each other in the two structures, as shown in Figure 4d. The iron and the two NE2 atoms of the axial ligands His39, His63 are located almost in a straight line in Lb_5 structure and the angle His39 NE2 – Fe – His63 NE2 is slightly smaller in Tb_5 (Table IVa). The distances between the atoms NE2 of His39 and His63 are 4.09 Å in both the Tb_5 and Lb_5. These data indicate that the binding of iron to the two axial imidazole rings are basically the same in Tb5 and Lb5. The side chain conformations of one of the axial ligands are

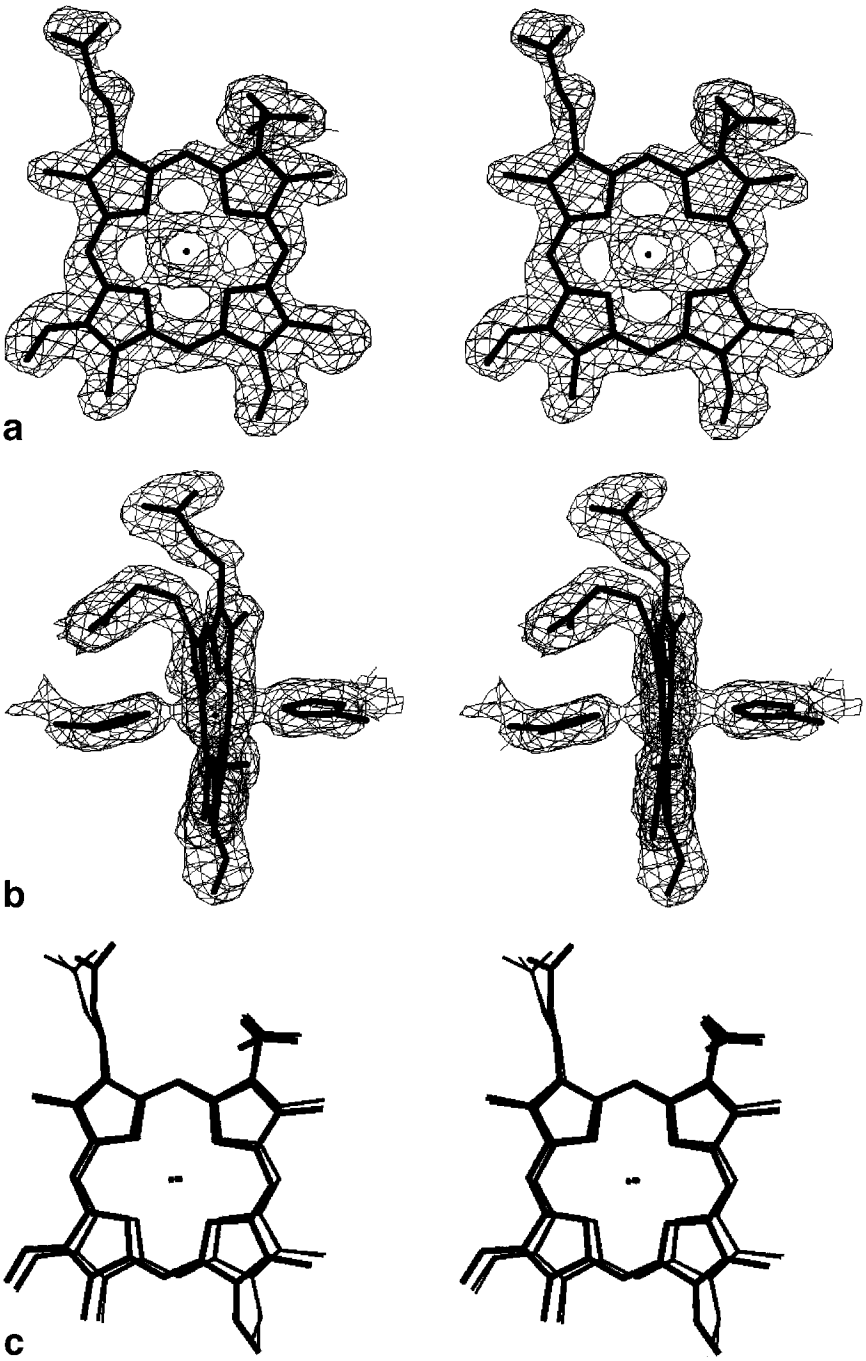

Fig. 4. **a:** The (2Fo-Fc) electron density of heme, calculated with the final model of the Tb_5 structure and contoured at 1.0σ. **b:** The (2Fo-Fc) electron density of heme and the two axial ligands, His39, His63, calculated with the final model of the Tb_5 structure and contoured at 1.0 σ. **c:** Heme of Tb_5, superimposed with those of Lb_5 and Val61His. Lb_5, Tb_5, and Val61His are shown in thick, medium, and thin lines, respectively. **d:** Heme, His39 and His63 of Tb_5, superimposed with those of Lb_5 and Val61His mutant. Tb_5 is shown in blue, Lb_5 in red and Val61His in white.

slightly different in the two structures, which is mainly attributed to the shift of helix V. The shift of iron between the two structures is 0.23 Å, and the conformational difference of heme itself between the two structures does not influence the coordination of the iron to the axial ligands.

The average iron-histidine ligand coordination distance in Tb_5 is the same as that in Lb_5. In order to confirm this result, the restraint for this coordination distance was changed in the range of 2.5–2.0 Å as a test using CNS program, which gave the refined Fe-His39/His63 distances in the range of 1.98–2.16 Å, indicating that the different restraints do not make much difference in the results.

The differences in the conformations of some side chains in the molecular surface region of Tb_5 from those of Lb_5 are also related to the different crystal packing. For example, the irregular hydrogen bonding pattern of helix I of Tb_5 differs from that of Lb_5, as described above, which can be ascribed to the crystal packing, i.e., the Gln13 of Tb_5 is located in the molecular surface region, and it would conflict with a symmetry-related molecule if its side chain was in the same conformation as that in Lb_5.

Figure 4. (Continued.)

TABLE IV a: The Distances and Angles Related to the Coordination of Iron to Axial Ligands in Tb_5, Lb_5, and Val61His

		Distance (Å)		
Atom 1	Atom 2	Tb_5	Lb_5^7	Val61His
Fe	His39 NE2	2.06	2.07	2.11
Fe	His63 NE2	2.03	2.00	2.08
His39 CA	His63 CA	11.80	11.66	11.88
His39 NE2	His63 NE2	4.09	4.09	4.18

			Angle (°)		
Atom 1	Atom 2	Atom 3	Tb_5	Lb_5^7	Val61His
His39 NE2	Fe	His63 NE2	174.98	177.96	173.40

b: Hydrogen Bond Interactions of the Solvent Network Close to Heme With the Surrounding Atoms

Atom 1	Atom 2	Distance (Å)
Wat319 O	Heme O1A	2.77
Wat319 O	Tyr27 OH(number 3)	2.58
Wat319 O	Wat343 O	2.97
Wat343 O	Ser64 OG	3.41
Wat343 O	Arg84 OT1 (number 3)	2.55
Wat320 O	Arg84 OT1 (number 3)	2.73
Wat320 O	Tyr27 OH (number 3)	2.65
Wat320 O	Asp66 OD2	3.19

Symmetry operator: number 3 −X + 1/2, Y + 1/2, −Z.

TABLE V. Intermolecular Hydrogen Bond Interactions†

Atom 1	Atom 2 (number)	Distance (Å)
Ala3 N	Glu11 OE1 (1)	2.46
Val4 N	Tyr6 O (1)	3.17
Val4 O	Tyr6 N (1)	3.05
Ser18 N	Asp83 OD1 (2)	2.89
Ser18 OG	Asp83 OD1 (2)	3.35
Ser18 OG	Leu9 N (2)	3.20
Ser18 OG	Glu10 N (2)	3.08
Ser18 OG	Asp83 OD2(2)	2.59
Lys34 NZ	His63 O (3)	3.17
Glu38 OE1	Lys28 NZ (3)	2.53

†The intermolecular interactions bridged by the water molecules were not included. Symmetry operators: number 1 −X + 1, Y, −Z + 1; number 2 −X + 1/2, Y + 1/2, −Z + 1; number 3 −X + 1/2, Y + 1/2, −Z.

The above-mentioned water network close to the heme in the Tb_5 structure does not exist in Lb_5 structure. On the other hand, a solvent network near the heme pocket, which interacts with Ser64 and both the propionates of heme, was reported in the Lb_5 structure.[7] However, none of those solvent molecules of Lb_5 can be found in the Tb_5 structure. The water networks in both structures involve intermolecular interactions, so that it is reasonable that Tb_5 and Lb_5 structures contain different water networks.

In addition to the different crystal packing, the shorter polypeptide chain at the C-terminus of Tb_5 than Lb_5 might be another factor to influence the tertiary structure directly or through intermolecular interactions. However, the six C-terminal residues were not determined in the Lb_5 structure[7]; therefore, it is impossible to discuss these influences, and the interactions involving the C-terminal segment of Lb_5 may be weak since this segment is probably disordered.

The Structural Comparison of the Wild-Type Tb_5 With Val61His Mutant

The conserved residue Val61 is located at the rim of the heme pocket (Fig. 1). The mutation from Val61 to His61 results in a positive shift of the redox potential by 21 mV and a decrease of the stability of the protein against heat and denaturant urea. The effect of the mutation of this

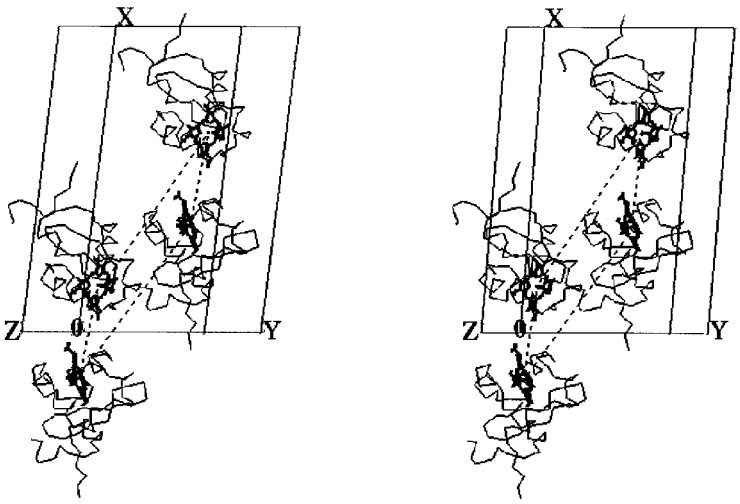

Fig. 5. Four symmetry-related molecules of Tb_5 with operators: X, Y, Z; −X, Y, −Z; X+1/2, Y+1/2, Z; and −X+1/2, Y+1/2, −Z. Cα backbones are shown in thin line and the heme groups are shown in thick line. The unit cell is also shown. The four Fe atoms are arranged as a parallelogram, and its long and short sides are 40.7 Å and 24.0 Å long, respectively.

residue on the structure, stability and redox potential have been discussed previously based on the structural comparison of Val61His with Lb_5.[13] Since the recombinant wild-type Tb_5 structure has been determined now, we can compare the further refined structure of Val61His with Tb_5 and make further discussion.

Tb_5 and its Val61His mutant are very similar to each other in their overall structures and heme binding, as described above. However, when the Val61His mutant is compared with Tb_5, the local structural changes can be observed at the mutation site.

The side chain of Val 61 in wild-type Tb_5 points toward the heme from the rim of the heme pocket, with the shortest distance of 4.15 Å to heme atoms. Its isopropyl group could act as a "gate" that restricts the access of solvent molecules from the top of the pocket into the heme pocket. When the residue Val61 is mutated to His61, the side chain of His61 points away from the heme pocket and extends into the solvent region. The Cα and Cβ atoms of this residue move toward heme plane by 0.24 Å and 0.25 Å respectively (Fig. 3). The position of the Cγ atom of His61 in the mutant is close to one of the two Cγ atoms of Val61 in Tb_5, and the remainder of the His61 side chain is located completely out of the heme pocket. The position of the other Cγ atom of Val61 in Tb_5 is not occupied when the valine is mutated to histidine, suggesting that the mutation from Val61 to His61 should probably lead to the opening of the gate formed by Val61. In the Val61His mutant structure, two solvent molecules are hydrogen bonded to the carboxyl oxygen of the main chain and the nitrogen atom NE2 of the side chain after Val61 is mutated to His61. On the other hand, the bulky imidazole ring of His61 makes a dihedral angle of approximately 45° with the mean plane of the heme and might form a new "gate" on the side way of the heme pocket. Therefore, the mutation from Val61 to His61 probably disturbs the micro-environment in the heme pocket and influences the accessibility of solvent molecules to the heme pocket. This disturbance and the alteration of the hydrophobicity of the heme pocket, along with the introduction of the positive charge, probably account for the effects of this mutation on the stability and the redox potential of cytochrome b_5.[13]

The coordination distances from iron to the two imidazole ligands in Val61His are 2.11 Å and 2.08 Å, respectively, only 0.05 Å longer than those in Tb_5 and Lb_5, as shown in Table IVa. It can be concluded that the mutation from Val61 to His61 does not obviously influence the binding of the two axial ligands to the heme. One of the two propionate groups and one of the two vinyl groups of the heme show flexible conformations in the Lb_5, Tb_5 and Val61His structures (Fig. 4c,d). However, the positions of the Cβ atoms of the vinyl group is close to each other when the three structures are superimposed.

The Structural Comparison of Microsomal Cytochrome b_5 With Its Homologous Proteins

Microsomal cytochrome b_5 shares high sequence homology not only with OMb_5, but also with the heme-containing "b_2 core" of flavocytochrome b_2 and the cytochrome b fragment of nitrate reductase.[24–27]

The sequence homology between OMb_5 and microsomal cytochrome b_5 is 58%, and their overall three-dimensional structures are almost identical with each other.[11] The comparison of OMb_5[11] with Lb_5 structures shows a rotation of heme about the normal of the mean plane by a small angle in the direction opposite to that of Tb_5 from the Lb_5 heme. Since the OMb_5 structure was reported at medium resolution, the detailed structural comparison of Tb_5 with OMb_5 will not been discussed.

The three-dimensional structure of flavocytochrome b_2 from baker's yeast was previously determined at 2.4 Å resolution.[28,29] Its cytochrome domain, referred to as the "b_2 core," shares the common "cytochrome b_5 fold" with Lb_5. However, its heme exhibits somewhat different conformation and orientation from those of Lb_5, with an approximately 30° rotation of the heme about the normal of the heme plane and the both propionates of the former are fully extended.

The crystal structure of the FAD-binding fragment, referred to as cytochrome b reductase fragment, of corn

nitrate reductase was reported at 2.5 Å resolution.[30] Based on this structure the three-dimensional structure of the heme-binding domain, referred to as the cytochrome *b* fragment, of this enzyme was built by computer modeling, and its interactions with the cytochrome *b* reductase fragment were also studied. It was shown that one of the two propionates, the one corresponding to the flexible propionate in microsomal cytochrome b_5, is probably involved in the domain-domain interactions.

This is the first report on the structure of the trypsin-solubilized fragment of cytochrome b_5. A series of mutants of Tb_5 have been prepared, and their functions are being studied. The determination of their structures is in progress and the structures will be compared with the wild-type Tb_5 structure, which may shed a new light on the detailed structure-function relationship of cytochrome b_5.

ACKNOWLEDGMENTS

We are grateful to Prof. Li-wen Niu, Prof. Mai-kun Teng and Dr. Xue-yong Zhu of the University of Science and Technology of China for their support and help with the X-ray data collection.

REFERENCES

1. Mathews FS. The structure, function and evolution of cytochromes. Prog Biophys Mol Biol 1985;45:1–56.
2. Mathews FS, Czerwinski EW, Argos P. The X-ray crystallographic structure of calf liver cytochrome b_5. In: Dolphin D, editors. The porphyrin, vol VII. New York: Academic Press, Inc.; 1979. p 107–147.
3. Spatz L, Strittmatter P. A form of cytochrome b_5 that contains an additional hydrophobic sequence of 40 amino acid residues. Proc Natl Acad Sci USA 1971;68:1042–1046.
4. Dailey HA, Strittmatter P. Modification and identification of cytochrome b_5 carboxyl groups involved in protein-protein interaction with cytochrome b_5 reductase. J Biol Chem 1979;254:5388–5396.
5. Mathews FS, Levine M, Argos P. Three-dimensional Fourier synthesis of calf liver cytochrome b_5 at 2.8 Å resolution. J Mol Biol 1972;64:449–464.
6. Mathews FS, Argos P, Levine M. Structure of cytochrome b_5 at 2.0 Å resolution. Cold Spring Harbor Quant Biol 1971;36:387–395.
7. Durley RCE, Mathews FS. Refinement and structural analysis of bovine cytochrome b_5 at 1.5 Å resolution. Acta Crystallogr D Biol Crystallogr 1996;52:65–76.
8. Salemme FR. An hypothetical structure for an intermolecular electron transfer complex of cytochrome c and b_5. J Mol Biol 1976;102:563–568.
9. Northrup SH, Thomasson KA, Miller CM, et al. Effects of charged amino acid mutations on the bimolecular kinetics of reduction of yeast iso-1-ferricytochrome c by bovine ferrocytochrome b_5. Biochemistry 1993;32:6613–6623.
10. Guillemette JG, Barker PD, Eltis LD, et al. Analysis of the bimolecular reduction of ferricytochrome c by ferrocytochrome b_5 through mutagenesis and molecular modeling. Biochimie 1994;76:592–604.
11. Rodriguez-Maranon MJ, Qiu F, Stark RE, et al. ^{13}C NMR spectroscopic and X-ray crystallographic study of the role played by mitochondrial cytochrome b_5 heme propionates in the electrostatic binding to cytochrome c. Biochemistry 1996;35:16378–16390.
12. Rivera M, Seetharaman R, Girdhar D, et al. The reduction potential of cytochrome b_5 is modulated by its exposed heme edge. Biochemistry 1998;37:1485–1494.
13. Xue L-L, Wang Y-H, Xie Y, et al. Effect of mutation at Valine 61 on the three-dimensional structure, stability, and redox potential of cytochrome b_5. Biochemistry 1999;38:11961–11972.
14. Funk WD, Lo TP, Mauk MR, et al. Mutagenic, electrochemical and crystallographic investigation of the cytochrome b_5 oxidation-reduction equilibrium: involvement of asparagine-57, serinee-64, and heme propionate-7. Biochemistry 1990;29:5500–5508.
15. Sambrook J, Fritsch EF, Maniatis T. Molecular cloning: a laboratory manual. 2nd edition. Cold Spring Harbor, NY: Cold Spring Harbor Laboratory Press; 1989.
16. Sanger F, Nicklen S, Coulson AR. DNA sequencing with chain-terminating inhibitors. Proc Natl Acad Sci USA 1977;74:5463–5467.
17. Mattehws BW. Solvent content of protein crystals. J Mol Biol 1968;33:491–497.
18. Otwinowski Z, Minor W. Processing of X-ray diffraction data collected in oscillation mode. Methods Enzymol 1997;276:307–326.
19. Brunger AT. X-PLOR: A system for X-ray crystallography and NMR, version 3.1. New Haven: Yale University Press; 1992.
20. Brunger AT, Adams PD, Clore GM, et al. Crystallography and NMR System (CNS): a new software system for macromolecular structure determination. Acta Crystllogr 1998;D54:905–921.
21. Roussel A, Cambillau C. TURBO-FRODO, Silicon Graphics partner geometry dictionary. Silicon Graphics, Inc., editors; 1991.
22. Morris AL, MacArthur MW, Hutchinson EG, Thornton JM. Stereochemical quality of protein structure coordinates. Proteins: Struct Funct Genet 1992;12:345–364.
23. Luzzati PV. Traitment statistique des erreurs dans la determination des structures cristallines. Acta Crystallogr 1952;5:802–810.
24. Ozols J, Strittmatter, P. Correction of the amino acid sequence of calf liver microsomal cytochrome b_5. J Biol Chem 1969;244:6617–6618.
25. Lederer F, Ghrir R, Guiard B, Cortial S, Ito A. Two homologous cytochrome b_5 in a single cell. Eur J Biochem 1983;132:95–102.
26. Guiard B, Groudinsky O, Lederer F. Homology between bakers' yeast cytochrome b_2 and liver microsomal cytochrome b_5. Proc Natl Acad Sci USA 1974;71:2539–2543.
27. Le K H D, Lederer F. On the presence of a heme-binding domain homologous to cytochrome b_5 in *Neurospora Crassa* assimilatory nitrate reductase. EMBO J 1983;2:1909–1914.
28. Xia Z-X, Shamala N, Bethge P, et al. Three-dimensional structure of flavocytochrome b_2 from baker's yeast at 3.0 Å resolution. Proc Natl Acad Sci USA 1987;84:2629–2633.
29. Xia Z-X, Mathews FS. Molecular structure of flavocytochrome b_2 at 2.4 Å resolution. J Mol Biol 1990;212:837–863.
30. Lu G, Lindqvist Y, Schneider G, Dwivedi U, Campbell W. Structural studies on corn nitrate reductase: refined structure of the cytochrome *b* reductase fragment at 2.5 Å, its ADP complex and an active-site mutant and modeling of the cytochrome *b* domain. J Mol Biol 1995;248:931–948.